Electronic Supplementary Material (ESI) for Journal of Materials Chemistry A.

Supporting Information

A sustainable approach to hierarchically porous carbons from tannic acid and their utilization in supercapacitive energy storage

Noel Díez, Guillermo A. Ferrero, Marta Sevilla, Antonio B. Fuertes*

Instituto Nacional del Carbón (CSIC), Fco. Pintado Fe 26, Oviedo 33011, Spain

*Corresponding author: abefu@incar.csic.es

Table S1. Chemical composition of the hierarchically porous carbons.

Sample code	Elemental composition (wt.%)					$(O/C)_{at}$[a]
	C	H	N	S	O	
CK-750	90.9	0.2	0.1	0.0	8.9	0.07
CK-800	93.2	0.2	0.1	0.0	6.5	0.05
CK-850	93.8	0.1	0.2	0.0	6.1	0.05
CK-900	93.5	0.1	0.3	0.0	6.2	0.05

[a] O/C atomic ratio.

Table S2. Textural properties and yield of tannic acid-derived carbons produced by a variety of conditions.

Sample code	Activating agent/template (wt. ratio)[a]	Textural properties			Yield[b] (%)
		S_{BET} (m^2 g^{-1})	V_{Total} (cm^3 g^{-1})	$V_{<2nm}$ (cm^3 g^{-1})	
TK	-/KCl (0/6.7)	510	0.48	0.16	26.1
CK	K_2CO_3/- (1/0)	1770	0.86	0.64	35.2
BK	$KHCO_3$/KCl (1/6.7)	2180	0.91	0.82	36.3
OK	$K_2C_2O_4$/KCl (1/6.7)	1990	0.84	0.72	38.7
CK-N	K_2CO_3/NaCl (1/6.7)	1890	0.91	0.69	35.0
CK-C	K_2CO_3/Na_2CO_3 (1/6.7)	1830	0.95	0.68	32.4
CK-F	K_2CO_3/KCl (1/6.7)	2340	0.98	0.86	36.1
CK-M	K_2CO_3/KCl (1/6.7)	2130	0.87	0.78	35.2

[a] Weight ratio with respect to 1 part of tannic acid.
[b] Yield calculated by dividing the weight of porous carbon by the weight of tannic acid in the mixture prior to pyrolysis.

Table S3. Textural properties and carbon yield of porous carbons obtained by using different biomass-based carbon precursors and activating agents.

Carbon precursor	Activating agent	Textural properties		Carbon yield[a] (%)	Reference
		S_{BET} (m^2 g^{-1})	V_{Total} (cm^3 g^{-1})		
Tannic acid	K_2CO_3	2740	1.39	32.1	[This work]
Lignin	K_2CO_3	1950	0.93	39.0	[37]
Waste tea	K_2CO_3	1722	0.95	15.9	[40]
Coconut shell	K_2CO_3	1430	0.65	48.0	[41]
Chickpea husk	K_2CO_3	1780	0.65	13.0	[42]
Palm shell	K_2CO_3	1170	-	19.0	[43]
Rice husks	K_2CO_3	1165	0.78	14.2	[44]
Tobacco stems	K_2CO_3	2557	1.65	16.7	[45]
Tannin-F hydrogel	KOH	1800	0.65	21.0	[31]
Sugar cane pulp	KOH	2910	2.05	11.0	[7]
Lignite	KOH	2810	1.35	9.7	[6]
Gulfweed	KOH	2862	1.62	31.4	[5]
Glucose	KNO_3	1912	0.93	9.1	[46]
Glucosamine	$K_2C_2O_4$	2680	1.49	11	[47]
soya flour	$K_2C_2O_4$	2924	2.15	5.0	[47]
Sodium Glutamate	none	1010	0.56	33.0	[22]

[a] Yield calculated by dividing the weight of porous carbon by the weight of biomass-based precursor.

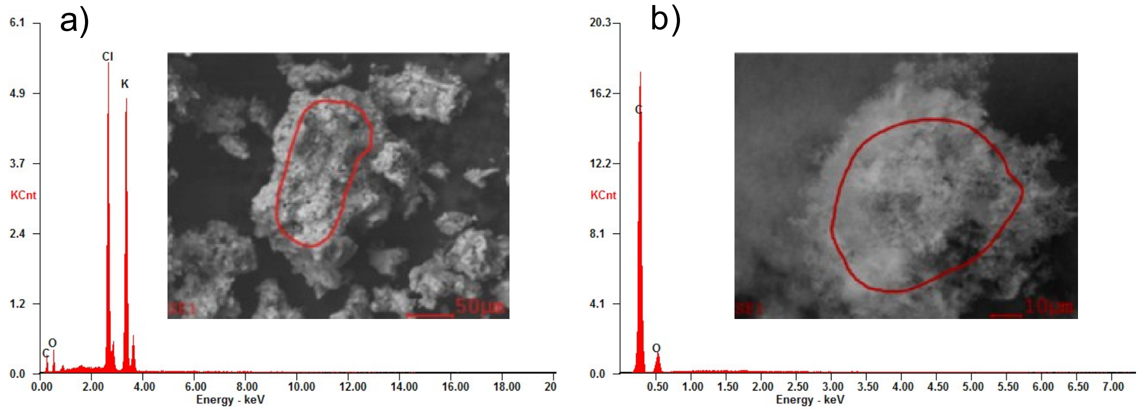

Figure S1. EDX analysis of a carbonized product (a) before and (b) after washing.

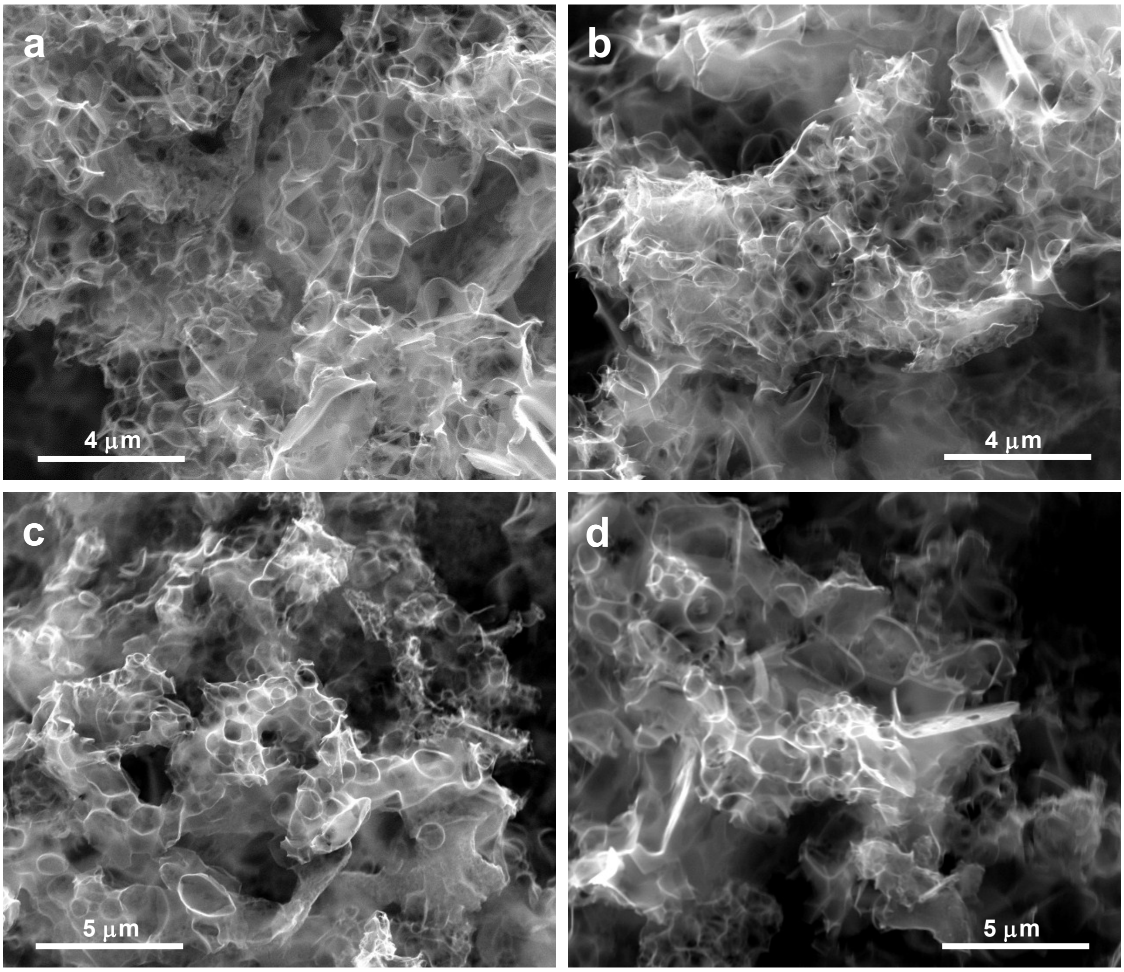

Figure S2. SEM images of CK-750 (a), CK-800 (b), CK-850 (c) and CK-900 (d).

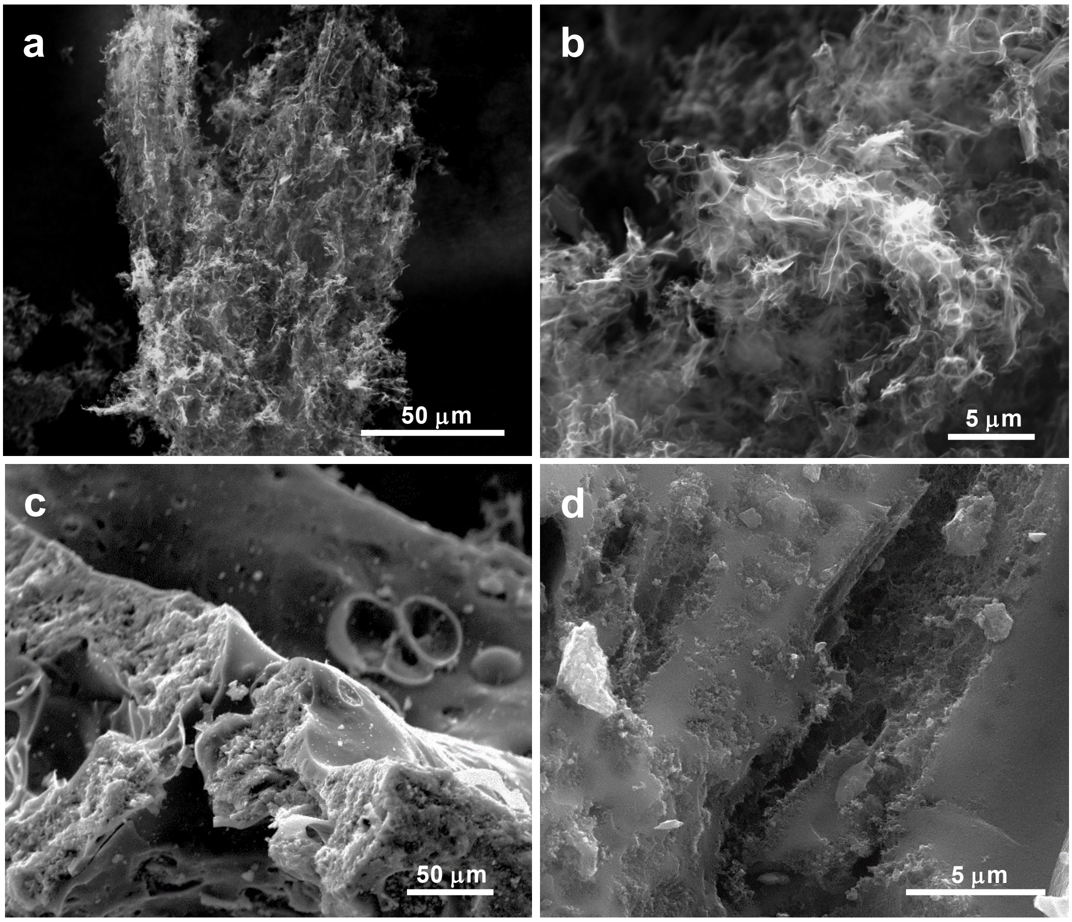

Figure S3. SEM images of sample TK prepared in the absence of K_2CO_3 (a and b) and CK carbon obtained in the absence of KCl (c and d).

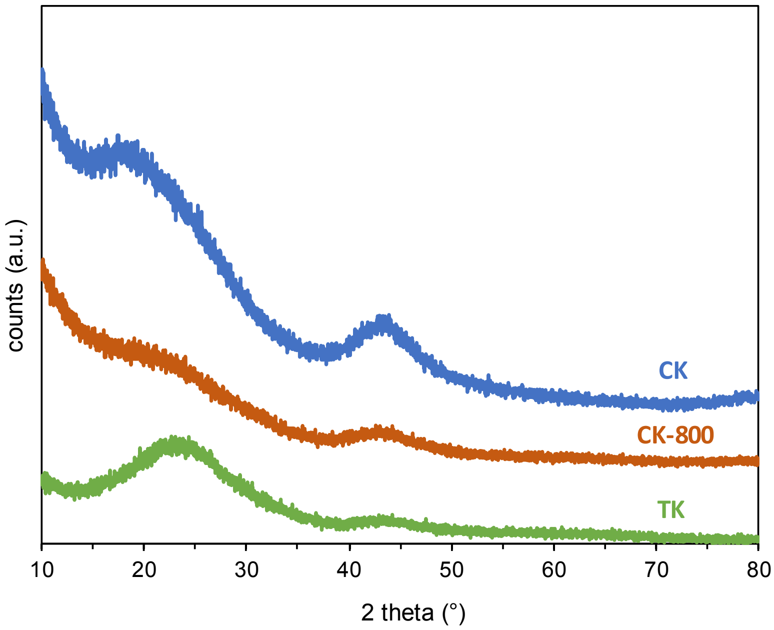

Figure S4. XRD patterns of carbons prepared from tannic acid and KCl (TK), tannic acid and K_2CO_3 (CK) and the ternary mixture (CK-800) using the same carbonization temperature (800 ºC).

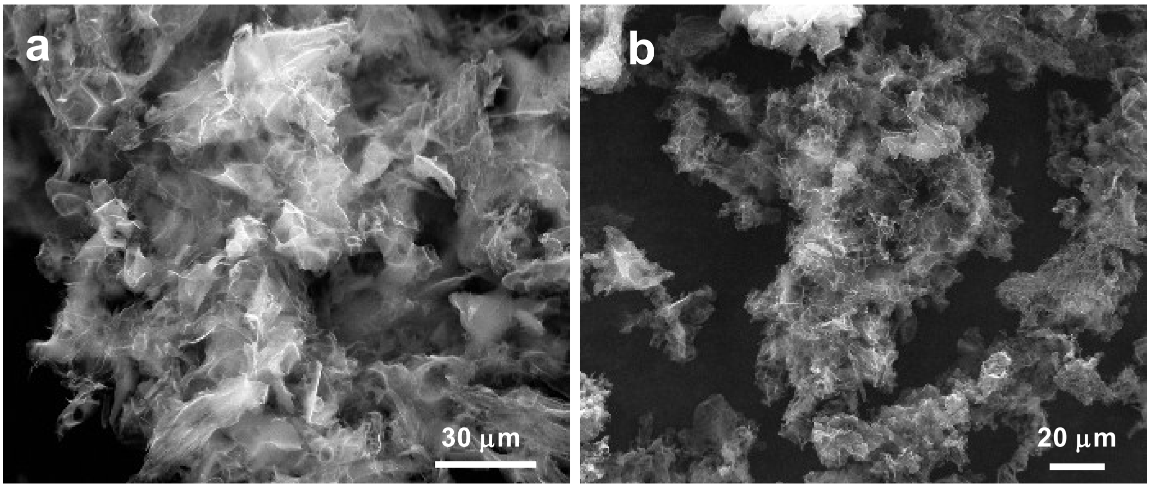

Figure S5. SEM images of BK (a) and OK (b) carbons.

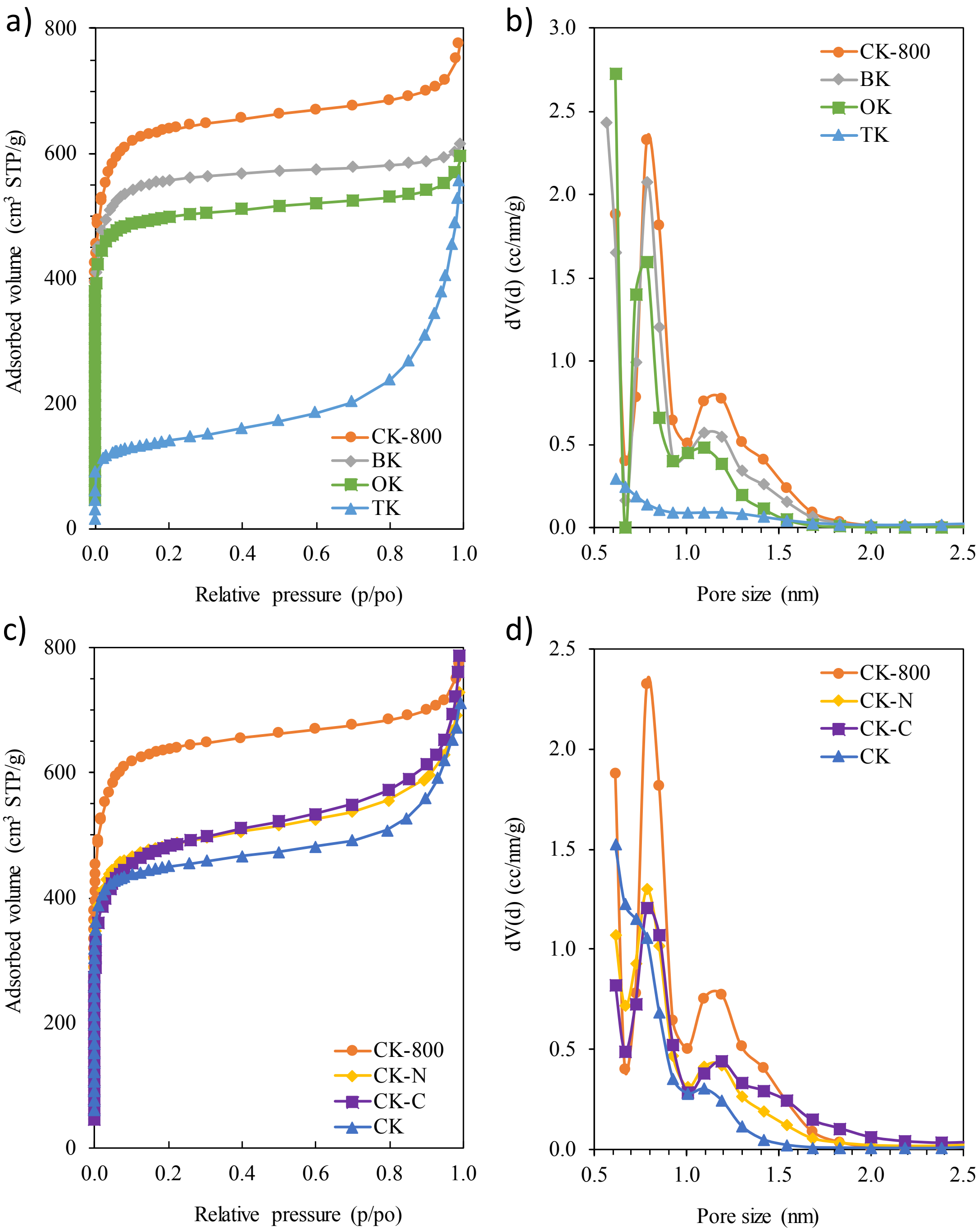

Figure S6. N_2 adsorption isotherms (a) and pore size distributions (b) of carbons prepared at 800 ºC using K_2CO_3, $KHCO_3$, $K_2C_2O_4$ and no activating agent. N_2 adsorption isotherms (c) and pore size distributions (d) of carbons prepared at 800 ºC using K_2CO_3, Na_2CO_3, NaCl and no salt template.

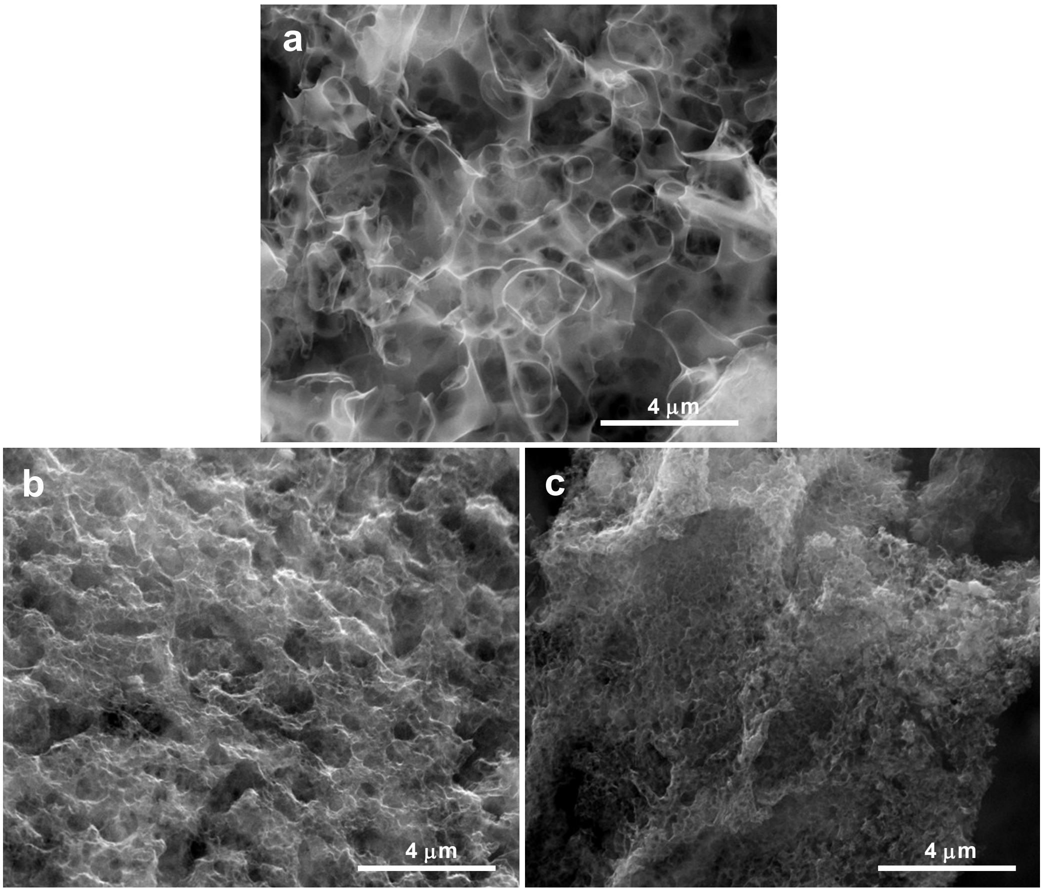

Figure S7. SEM images of CK-800 (a), CK-C (b) and CK-N (c) carbons.

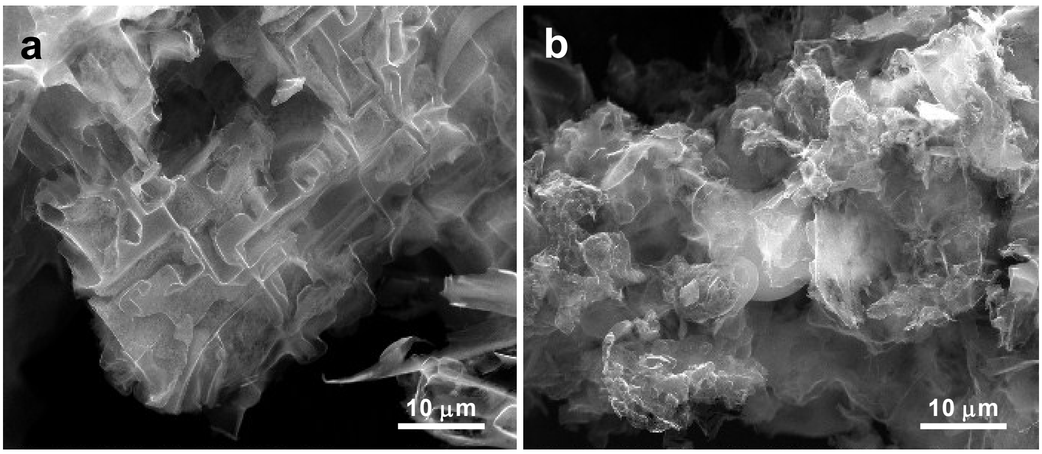

Figure S8. SEM images of CK-F (a) and CK-M (b) carbons.

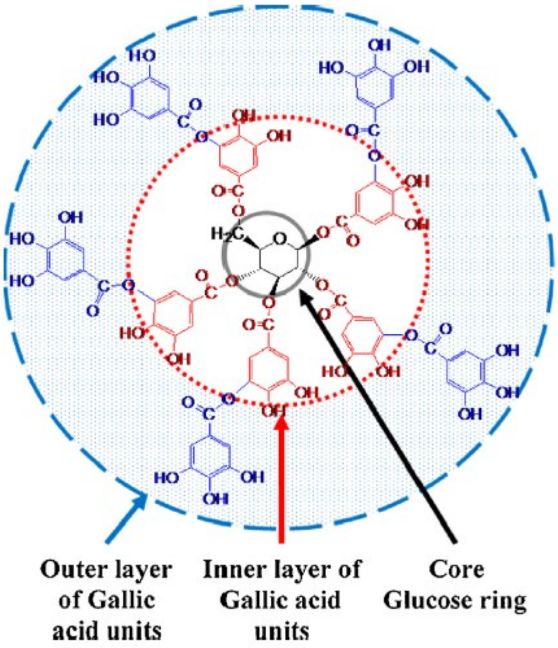

Figure S9. Chemical structure of tannic acid. Figure reproduced with permission.[1] Copyright, Elsevier, 2015.

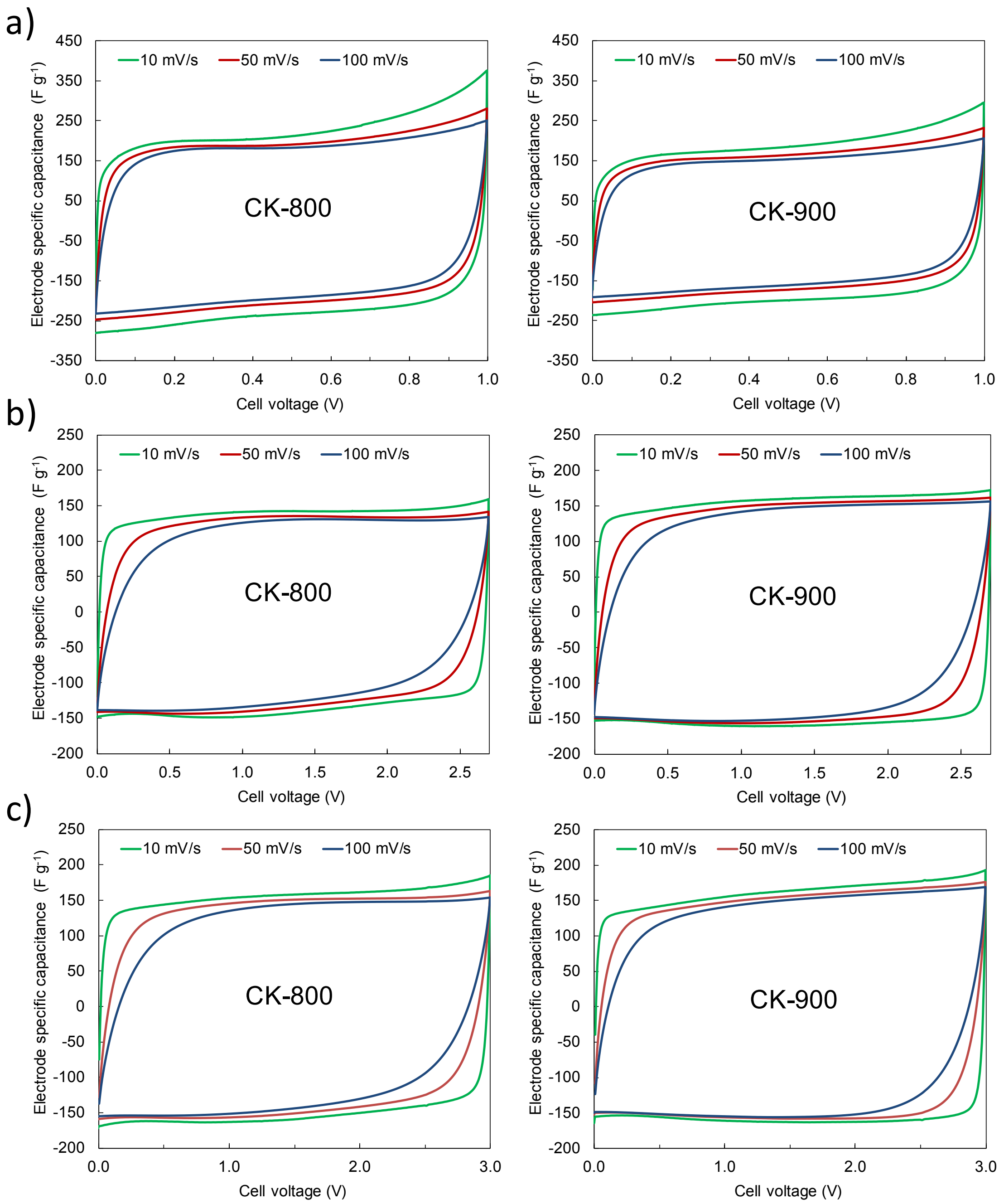

Figure S10. Cyclic voltammograms at different scan rates of the porous carbons in (a) 1M H_2SO_4, (b) 1 M $TEABF_4$ and (c) EMImTFSI/AN.

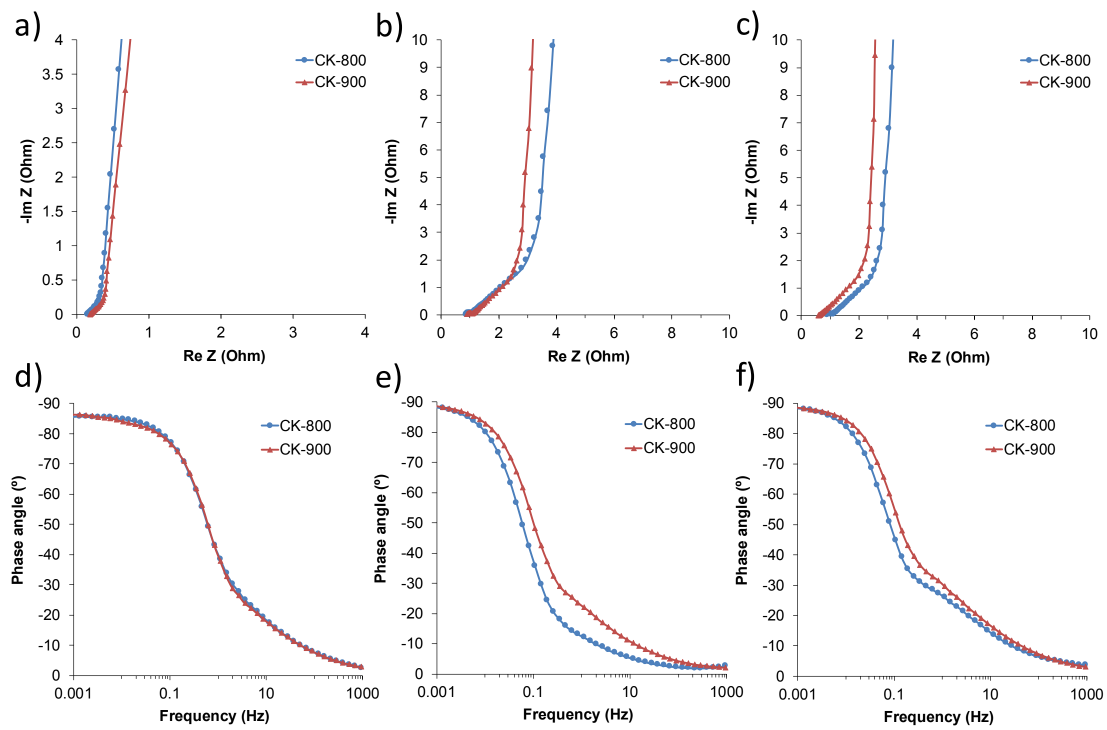

Figure S11. Nyquist plots (above) and Bode plots (below) for the porous carbons in 1 M H_2SO_4 (a and d), 1 M $TEABF_4$ (b and e) and EMIMTFSI/AN (c and f).

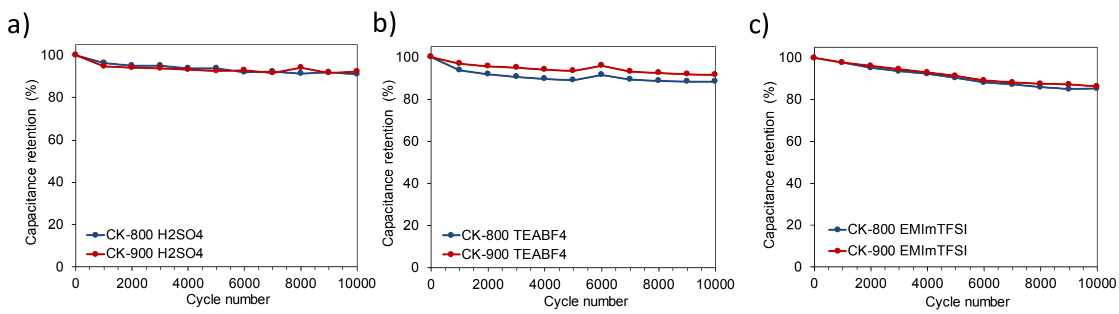

Figure S12. Cycling stability of the electrodes in (a) 1 M H_2SO_4, (b) 1 M $TEABF_4$ and (c) EMIMTFSI/AN.

1. Z. Xia, A. Singh, W. Kiratitanavit, R. Mosurkal, J. Kumar and R. Nagarajan, *Thermochim. Acta*, 2015, **605**, 77-85.